Langmuir

Article

pubs.acs.org/Langmuir

Surfactant-Induced Phases in Water-Supported Alkane Monolayers: I. Thermodynamics

Shai Yefet,[†,§] Eli Sloutskin,[†,§] Lilach Tamam,[†,∥] Zvi Sapir,[†,⊥] Asaf Cohen,[†] Moshe Deutsch,*[,†] and Benjamin M. Ocko*[,‡]

[†]Physics Department and Institute of Nanotechnology, Bar-Ilan University, Ramat-Gan 52900, Israel

[‡]Condensed Matter Physics & Materials Sciences Department, Brookhaven National Laboratory, Upton, New York 11973, United States

ABSTRACT: Alkanes longer than $n = 6$ carbons do not spread on the water surface, but condense in a macroscopic lens. However, adding trimethylammonium-based surfactants, C_mTAB, in submillimolar concentrations causes the alkanes to spread and form a single Langmuir−Gibbs (LG) monolayer of mixed alkanes and surfactant tails, which coexists with the alkane lenses. Upon cooling, this LG film surface-freezes at a temperature T_s above the bulk freezing temperature T_b. The thermodynamics of surface freezing (SF) of these LG films is studied by surface tension measurements for a range of alkanes ($n = 12-21$) and surfactant alkyl lengths ($m = 14, 16, 18$), at several concentrations c. The surface freezing range T_s-T_b observed is up to 25 °C, an order of magnitude larger than the temperature range of SF monolayers on the surface of pure alkane melts. The measured (n,T) surface phase diagram is accounted for well by a model based on mixtures' theory, which includes an interchange energy term ω. ω is found to be negative, implying attraction between unlike species, rather than the repulsion found for SF of binary alkane mixtures. Thus, the surfactant/alkane mixing is a necessary condition for the occurrence of SF in these LG films. The X-ray derived structure of the films is presented in an accompanying paper.

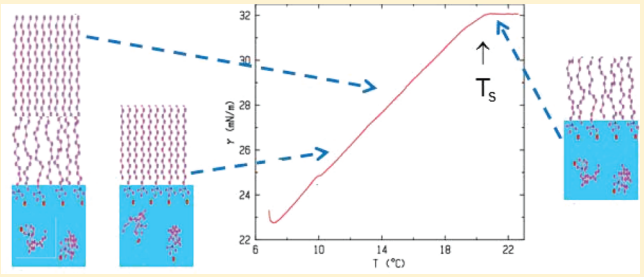

INTRODUCTION

Normal-alkanes, methyl (CH_3) terminated linear methylene (CH_2) chains ($CH_3(CH_2)_{n-2}CH_3$, denoted as C_n), are among the most basic building blocks of organic molecules. They are major constituents of lipids, surfactants, liquid crystals, polymers, and many other, more complex organic compounds.[1] Their properties strongly influence, and in many cases dominate, the properties and structure of their more complex host molecules. Therefore, their structure and properties have been studied extensively, with new, and often intriguing, results still being uncovered.[1−3] In spite of their simple molecular architecture, bulk alkanes were found to exhibit a rich phase diagram, with several distinct rotator and crystalline phases, both transient and stable.[2,4] Moreover, the liquid/vapor interface of alkane melts was found[5−7] to exhibit surface freezing (SF), an unusual effect where a crystalline surface monolayer of a pure alkane is found to coexist in thermodynamic equilibrium with the alkane's own underlying melt for a temperature range of up to ∼3° above the bulk freezing point T_b. This is in contrast with the vast majority of materials, where the excess surface entropy of the less confined surface molecules over that of the bulk molecules renders their melting temperature lower than that of the bulk. Hence, a liquid surface is expected to coexist with the underlying frozen bulk over some temperature range *below* T_b, an effect known as surface melting. While surface melting has indeed been observed in numerous solids,[8,9] SF has been observed only in pure alkanes and derivatives (semifluorinated alkanes, alcohols, α,ω-diols, polymers with alkyl side chains, etc.)[5−7,10,11] and their mixtures.[12] SF was also shown to occur in metallic glass-forming binary Au/Si alloys.[13]

A number of theoretical approaches have been used to explain the SF effect. These range from simple surface energy balance considerations,[14] a higher surface affinity of the CH_3 moiety,[15] to entropic surface layer stabilization by surface-normal molecular fluctuations[16] or a lowering of the molecule's internal energy by chain-end conformational disorder.[17] Several other analytical and simulational calculations have also been carried out.[18−20] However, in alkanes and their derivatives, no consensus has emerged as yet on the basic reasons for the occurrence of SF, rather than the expected surface melting.

SF was also explored at interfaces other than the free surface of alkane melts. At alkane/solid interfaces, no SF was found, although thin alkane films supported on solid interfaces show effects which are related to SF,[21,22] and bulk *alcohols* exhibit SF at the melt/sapphire interface.[23] At the liquid/liquid interface of alkane and water, measurements[24] failed to detect any temperature-driven structural transition akin to SF above T_b. However, adding submillimolar concentrations of the cationic surfactants TTAB (tetradecyltrimethylammonium bromide, *m*

Received: April 23, 2014
Revised: June 9, 2014
Published: June 11, 2014

= 14), CTAB (cetyltrimethylammonium bromide, m = 16), or STAB (stearyltrimethylammonium bromide, m = 18) to the water was demonstrated to induce the formation of a mixed monolayer of alkanes and surfactant tails at the interface between the two bulks.[25,26] This mixed monolayer undergoes a (interfacial) freezing transition at up to ∼15 °C above T_b, depending on the alkane and surfactant lengths, n and m, respectively, and the bulk concentration of the surfactant.[25−27] This interfacial freezing effect occurs only for alkane lengths up to $n = m - 1$.

Effects similar to those discussed in the previous paragraph were also found to occur at the free surface of water.[27,28] Alkanes, the archetypical hydrophobes, do not spread on the free surface of water when their lengths exceed n = 6 carbons. When a droplet of such an alkane is placed on the pure water surface, it forms an isolated 3D lens in equilibrium with a coexisting dilute 2D gas of alkane molecules, a phase denoted as partial wetting.[29,30] However, very dilute concentration of one of the surfactants mentioned above induces a transition to a pseudopartial wetting phase, where a single monolayer of mixed alkanes and surfactants' tails, called a Langmuir−Gibbs (LG) monolayer,[27] forms at the surface of the solution, and coexists with the excess alkane molecules residing in the lens.[28,29,31] The long-range van der Waals interaction across the LG film (the disjoining pressure[29,32]), which is compressive due to the positive sign of the Hamaker constant for alkanes on water at room temperature, reduces its thickness to below 1 nm.

Ellipsometry[28] and sum-frequency vibrational spectroscopy[33] showed that, upon cooling, the mixed alkane/surfactant-tail LG film at the solution's surface undergoes a structural transition at some T_s to a dense phase in which the hydrocarbon chains assume an all-*trans* conformation and are oriented normal to the water surface. Our X-ray measurements[27] for CTAB revealed the sub-T_s phase to be a hexagonal 2D crystal of close-packed, surface-normal chains for all alkane lengths studied. However, for $n \leq m + 1$, the LG film consists of a single monolayer of mixed alkanes and surfactant tails, while for $n \geq m + 2$, a bilayer is formed in the SF phase, in which the lower monolayer consists of the disordered surfactant tails and the upper monolayer is a hexagonally packed 2D crystal consisting of extended, surface-normal, pure alkane molecules. That study also determined the surface (n,T) phase diagram of LG films of n = 12−21 alkanes on a CTAB (m = 16) solution for a single concentration, and presented a simple, mixtures'-theory-based thermodynamic model for its interpretation.

The few previous studies discussed above[28,27] do not address the surfactant length dependence or the concentration dependence of the surfactant-mediated SF effect, nor do they discuss in depth the phase diagram model and its underlying mixtures'-theory-based physics. We present here a detailed and systematic study of the thermodynamics and structure of surfactant-mediated SF at the free surface of a dilute aqueous surfactant solution for m = 14, 16, 18, n = 12−21, and a few surfactant concentrations. This paper presents measurements of the thermodynamics of these LG films. An accompanying paper[34] presents X-ray measurements of the LG films' structure above and below T_s. The broader range of these results allows a significantly deeper discussion of, and insight into, the physics dominating the SF transition and identifies the attractive interchange energy as the driving force behind the SF in these LG films.

EXPERIMENTAL SECTION

Materials and Procedures. The surfaces we study are notoriously sensitive to impurities in the chemicals used,[28,35] particularly to surface active ones, like alcohols, which, unfortunately, are a common impurity in the C_mTAB surfactants used here.[36,37] Thus, the highest-purity commercial materials were purchased, and further purified before use. Millipore water (18.2 Ω m) was used in the cleaning and for surfactant solution preparation. Purchased CTAB, STAB, and TTAB (> 98% purity) were recrystallized three times from a methanol/acetone solution.[36] Alkanes (≥ 99% purity) were purchased from Sigma-Aldrich-Fluka and percolated three times through activated basic alumina powder columns to remove polar impurities. Only glass and Teflon came in contact with the samples. Following measurements of the time stability of the surface tension of samples prepared using several different cleaning procedures, all pieces in contact with the sample were first cleaned by standard methods, followed by immersion in freshly prepared piranha solution (75% sulfuric acid + 25% hydrogen peroxide) for ∼5−10 min, then thoroughly rinsed in Millipore water, dried, and used immediately.

The alkanes were deposited at the solution surface by pipetting a few microliters of a freshly sonicated 1:10 (v/v) solution of alkane in chloroform (Aldrich, ≥ 99.9% pure, ethanol-satbilized). The exact amount deposited was found to be immaterial, and amounts of 3−12 μL yielded identical results. Similarly, variations in the alkane solution concentration from 1:5 to 1:20 yielded also identical results. As the alkane amount in the deposited solution far exceeded that required to form a single LG monolayer, the chloroform evaporation after deposition leaves a few tiny 3D alkane lenses in equilibrium with the LG monolayer. The surface area fraction occupied by these droplets is, however, negligible, and the surface can be considered to be fully covered by the LG monolayer.

Surface Tension Measurements. The temperature-dependent surface tension measurements were carried out by the Wilhelmy plate method,[6,26,38] using a computerized in-house constructed film balance.[7,26] A roughened glass Wilhelmy plate was employed, after checking that a platinum plate yielded identical results for several samples. The sample resided in a small glass beaker, sitting inside an all-metal cell, the temperature of which was controlled to ≤0.005 °C by a Lakeshore model 340 temperature controller using a 100 KΩ (at 25 °C) YSI high-sensitivity thermistor. This actively controlled cell resided inside another thick-walled, passive, metal cell. The Wilhelmy plate hangs from a thin wire, attached to an electronic balance, and passing through small holes in the tops of the inner and outer cells. The experiment is controlled by a computer which reads the force acting on the plate and the temperature, displays the results, and scans the temperature of the cell uni- or bidirectionally. Temperature scans were carried out stepwise at a rate of 0.03 °C/30 s.

RESULTS AND DISCUSSION

Surface Tension Curves. The surface tension $\gamma(T)$ is given by $\gamma(T) = (\varepsilon_s - \varepsilon_b) - T(S_s - S_b)$, where ε, S, b, and s denote energy, entropy, bulk, and surface, respectively. For liquids, $S_s > S_b$, yielding $d\gamma/dT < 0$, and thus, a monotonically decreasing curve with increasing T is expected. This is indeed observed in the measured $\gamma(T)$ of a bare CTAB solution shown in Figure 1a. In particular, no kinks or slope changes, which may indicate a surface ordering transition, are observed.[6] Upon depositing liquid alkane on the surface, a different temperature evolution results, demonstrated by the measured $\gamma(T)$ curve of C_{15} on a CTAB solution, shown in Figure 1b. Here, the sharp slope change occurring at some temperature is indicative of an ordering transition on the surface, since such a transition lowers S_s below S_b, and thus renders $d\gamma/dT > 0$. This slope change identifies the surface freezing temperature, T_s, and also yields the entropy loss upon surface freezing, $\Delta S_s \equiv S_{s,T>T_s} - S_{s,T<T_s} = d\gamma/dT_{T<T_s} - d\gamma/dT_{T>T_s}$.

dx.doi.org/10.1021/la501567s | Langmuir 2014, 30, 8000−8009

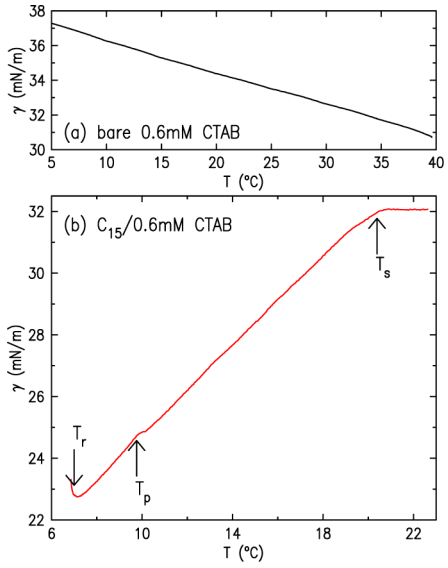

Figure 1. (a) Measured surface tension $\gamma(T)$ of 0.6 mM CTAB solution, before alkane deposition. Note the monotonic linear decrease with increasing temperature. (b) Typical measured $\gamma(T)$ curve of a C_{15} Langmuir–Gibbs film on 0.6 mM CTAB solution. The slope change at T_s is a macroscopic manifestation of the freezing of the LG film. The temperatures marked by arrows are discussed in the text.

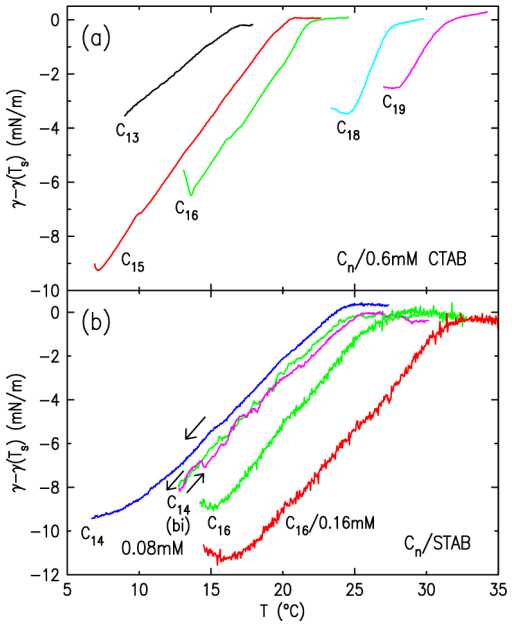

Figure 2. (a) Measured $\gamma(T)$ curves for LG films of the indicated alkanes on the surface of a 0.6 mM CTAB solution. (b) Measured $\gamma(T)$ curves, discussed in the text. From left: C_{14} on 0.08 mM STAB solution upshifted for clarity by 0.5 mN/m, same curve measured bidirectionally, and C_{16} on 0.08 mM and on 0.16 mM STAB solutions. Note that no temperature hysteresis is observed in the bidirectionally measured curve. Also note the T_s shift due to the different STAB concentrations of the (two rightmost) C_{16} curves.

For each alkane/surfactant combination, the ΔS_s value derived here from its $\gamma(T)$ curve, like that in Figure 1b, is very close to the ΔS_s value obtained for the same alkane from the freezing of a single surface monolayer of the melt.[6,7] This suggests that the slope changes observed here are also due to the freezing of single alkane monolayers, albeit at the surface of the surfactant solution, rather than that of a melt. This is indeed confirmed by our X-ray measurements, discussed in the accompanying paper,[34] which directly determine the layer's thickness. Note also that the measured $\gamma(T < T_s)$ exhibits two additional features, occurring at T_p (p for plateau) and T_r (r for rise). These features have no parallels in the surface freezing of alkane melts,[6,7] alkanols,[39] or mixtures,[12] where the corresponding $\gamma(T < T_s)$ are smooth, straight lines. These features indicate further changes in the surface structure, which will be discussed below.

Figure 2a shows a selection of measured $\gamma(T)$ curves for the indicated alkane lengths on a CTAB solution, measured in cooling. While the same general features, that is, a slope change at T_s and another at T_r, are observed, some more subtle variations can be observed. For example, the feature marked as T_p in Figure 1b is not observed for $C_n > 16$, the length of the alkyl moiety of the CTAB. Moreover, the $T > T_s$ slopes for the longer alkanes tend to also be positive, though small. A similar systematic change from a small negative slope to a small positive one at $T > T_s$ was also observed for bulk C_{14} on CTAB solution,[25] albeit as a function of increasing surfactant concentration. These effects in the liquid surface phase may indicate a trend of increasing order with n and c. Note also that several of the freezing transitions at T_s appear rounded, particularly for the longer alkanes, which have higher melting and T_s temperatures. This may be due to a slightly higher impurity contents of the longer alkane, resulting from a lower efficiency and a higher difficulty in cleaning these alkanes, which are solid at room temperature and require therefore a constant heating during alumina filtration. In cases of significant rounding of the transition in the measured $\gamma(T)$ curves, T_s was determined as the intersection of straight line sections fitted to the straight sections of the measured curve above and below the transition.

A few points worth noting are summarized in Figure 2b. Note first the $\gamma(T)$ measurement shown in the two leftmost curves. Following a full cooling T-scan of C_{14} on 0.08 mM STAB solution (blue curve), we have reheated above T_s, and repeated the cooling scan on the same sample (left green curve), stopping just before T_r and reversing the scan to a heating one (magenta curve). (For clarity, the blue curve was upshifted from the green and the magenta curves by 0.5 mN/m .) Within the fluctuations in the measured values, the two curves (green and magenta) coincide, indicating that although the surface freezing transition at T_s is first-order, as should be the case for any freezing transition, no temperature hysteresis is observed in this transition within our resolution. This agrees with the same conclusion derived for surface freezing in alkane melts where the monocomponent system is simpler, $\gamma(T)$ values fluctuate less, and the transition at T_s is sharper.[6,7] A second important point is demonstrated in the two rightmost $\gamma(T)$ curves, measured for the same alkane, C_{16}, but for two different-concentration STAB solutions. The different concentrations yield different STAB coverage at the surface, a different free energy balance, and hence a different T_s. This is discussed further below.

Several $\gamma(T)$ curves were measured for each sample, and a few different samples were measured for each C_n/surfactant combination. The quantities derived from these curves provided an average value and an uncertainty estimate for each quantity. These are summarized in Table 1.

Special Temperatures: T_r and T_p. In Figure 3, we compare the n-dependence of T_r and T_p with that of the bulk

dx.doi.org/10.1021/la501567s | Langmuir 2014, 30, 8000–8009

Table 1. Freezing Temperature (T_s) and Entropy Loss (ΔS_s in mJ/(m^2 K)) of C_n on Different Surfactants and Concentrations[a]

	TTAB						CTAB			STAB						
	1 mM			2 mM			0.6 mM			0.08 mM			0.16 mM			
n	T_s	ΔS_s	T_r	T_s	ΔS_s	T_r	T_s	ΔS_s	T_r	T_s	ΔS_s	T_r	T_s	ΔS_s	T_r	T_b
12							10.2									-9.6
13	3.6	0.55		4.5	0.5		15.1	0.52		19.3	0.64	10.0	20.8	0.68		-5.39
14	5.1	0.51	1.8	6.0	0.61		17.2	0.52		23.8	0.71		26.5	0.73		5.86
15	9.2	0.75	7.5	9.4	0.64	8.2	20.6	0.73	7.1	27.2	0.71		28.9	0.71		9.93
16	16.7	0.64	14.8	16.5	0.7	13.8	22.5	0.84	13.7	28.2	0.83	15.6	30.3	0.8		18.17
17	21.8	0.7	19.8	22.7	0.73	20.3	22.7	0.67	18	29.9	0.77		32.7	0.83		21.98
18	28.1	0.78	26.2	28.0	0.85	25.4	27.3		24.8	30.6	0.82	24.7	32.4	0.81		28.18
19	32.9	0.85	30.6	32.6	0.87	30.2	32.3		29.5	32.9	0.82	29.3	34.2	0.83	30.7	32.1
20							37.8	0.95	33.3	38.1	0.92	33.7	37.6	0.97	34.5	36.8
21				41.0	0.95	36.4				41.7	0.98	36.2	42.0	0.95	36.3	40.5

[a] T_r is defined as the temperature at which the surface tension starts rising again with decreasing temperature, after the linear decrease starting at the freezing point, T_s. T_b values are taken from Small.[1] All temperatures are in °C.

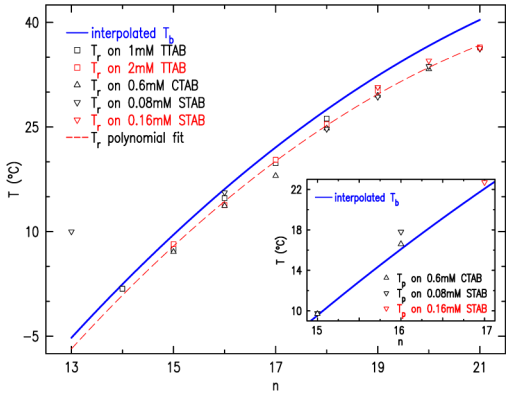

Figure 3. Comparison of the measured T_r (symbols) with the interpolated bulk freezing temperatures T_b (solid line) for all surfactants, concentrations, and alkane lengths studied. The dashed line is an ad hoc quadratic polynomial fit to the measured T_r. Inset: The same for T_p. For a discussion, see the text.

freezing temperature T_b for the three surfactants, at several concentrations. Our X-ray measurements,[34] and our previous work,[27] demonstrate that LG films freeze into a rotator phase for all n. Thus, to avoid odd−even effects on T_b, $T_b(n)$ values for even n (where the bulk freezes into a crystalline phase) were interpolated from $T_b(n)$ values of odd lengths n (where the bulk freezes into a rotator phase).[1] The coincidence of T_p, where observed, with T_b (inset) identifies it as the freezing temperature of the alkane lenses coexisting at the surface with the LG film. This also explains why T_p is observed only for $n \leq m + 1$: at higher n, T_b and thus T_p coincide with T_s. The values of, and trend followed by, T_r are more difficult to rationalize. T_r appears in almost all $\gamma(T)$ measurements as a rather abrupt change from the positive slope of the $\gamma(T < T_s)$ curve to a negative value (see Figure 1b). The magnitude of the slope change varies randomly with concentration, n and m. T_r itself shows, however, a systematic trend. As Figure 3 demonstrates, $T_r(n)$ follows $T_b(n)$ with an almost constant negative offset of 3−4 °C, with the offset increasing slightly with increasing n (or T). The dashed line in Figure 3, which is a fit of the measured $T_r(n,c)$ values in Table 1 by a quadratic polynomial, amply demonstrates this effect. A decrease in the slope indicates surface disordering, as discussed above. However, at $T_r < T_b < T_s$, the LG film and its coexisting alkane lenses are both solid; thus, a remelting of the LG film at this low temperature is an unlikely explanation for the disordering. We propose, therefore, that the disordering is due to a (partial) dewetting of the interface by the LG film, perhaps at the periphery of the lenses, with the alkane molecules migrating into the lenses. A possible decrease in the bulk entropy while that of the surface remains unchanged could also account for this effect. However, since the insoluble alkanes are excluded from the bulk subphase, this scenario could not explain why $T_r(n)$ follows so closely the alkanes' $T_b(n)$.

Entropy Loss upon Surface Freezing. The entropy losses upon surface freezing, $\Delta S_s(n)$, derived from the measured changes in $d\gamma(T)/dT$ at T_s are summarized in Figure 4. Within the scatter of the measured TTAB values in Figure 4a, ΔS_s exhibits a linear dependence on n, as expected,[6,7] and is independent of the surfactant concentration c. Thus, for TTAB and for STAB, measured each at two concentrations, the values for each n were averaged and plotted in Figure 4b. The resultant reduced scatter in the points reveals for STAB a new important feature: while $\Delta S_s(n)$ is indeed linear in n for both the frozen monolayer ($n \leq m + 1$) and frozen bilayer ($n \geq m + 2$) phases, $\Delta S_s(n)$ seems to have different slopes in the monolayer and bilayer phases. This is clearly observed in the fitted red dashed lines in Figure 4b. TTAB seems to show a similar two-slope n dependence (dashed black lines), although the slope in the monolayer phase here rests on two n values only. It is, therefore, much less prominent than the STAB behavior, particularly since the unaveraged points can be fitted reasonably well, within their scatter, by a single straight line for all n, as indeed done in Figure 4a. For CTAB, the measured $\Delta S_s(n)$ values are too few, particularly for $n \geq m + 2$, and too scattered to allow a similar analysis.

For the bilayer phase at $n \geq m + 2$, where only alkanes are included in the upper frozen layer but not surfactant tails, $\Delta S_s(n)$ exhibits nearly no dependence on m, as demonstrated by the near coincidence in Figure 4b of the dashed lines fitted to all three data sets. By contrast, for the monolayer phase, $n \leq m + 1$, the values of $\Delta S_s(n)$ show a strong m dependence. This is demonstrated in Figure 4b for $n = 13$, 14 where $\Delta S_s(n)$ is 30% higher for STAB than for TTAB. This can be rationalized by observing that in this phase the surfactant tails are included in the frozen layer, and the freezing out of their degrees of freedom should yield a larger $\Delta S_s(n)$ for the longer STAB than for the shorter TTAB.

dx.doi.org/10.1021/la501567s | Langmuir 2014, 30, 8000−8009

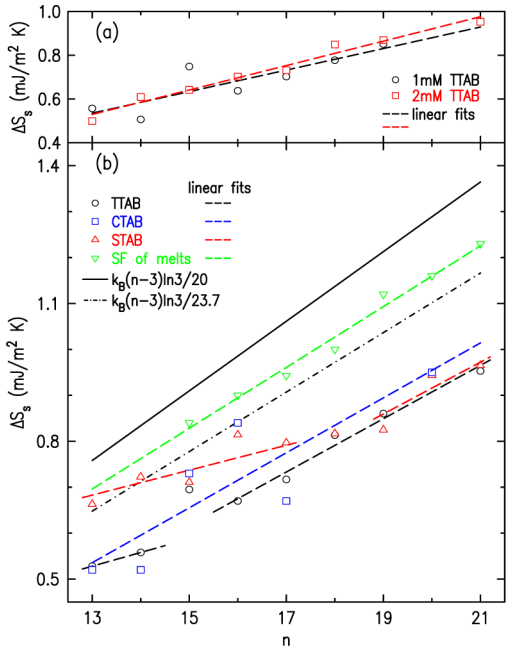

Figure 4. (a) Entropy loss upon surface freezing, ΔS_s, (symbols) derived from the slope change of the measured $\gamma(T)$ at T_s for LG films on TTAB, with linear fits to the points at each concentration (dashed lines). Note the linear increase with alkane length n, and the near independence of the TTAB concentration. (b) Same for TTAB (black), CTAB (blue), STAB (red), and SF of alkane melts[6,7] (green), along with linear fits to each data set (same-color dashed lines), in the monolayer and bilayer surface phases. Note the different slopes in the two phases for each surfactant. The black solid and dash-dot lines are a simple thermodynamic model for the freezing of a monolayer, discussed in the text.

The linear dependence of ΔS_s on n, in general, has been rationalized for SF of alkane melts[6,7] by considering the bond conformation statistics along the chain. The first two C−C bonds determine a reference plane for the conformations of subsequent bonds. All successive bonds can assume two *gauche* and one *trans* conformations relative to that plane, with the latter having the lowest energy.[40] Assuming that in the liquid phase a chain is completely flexible (kinked) and the three bond conformations occur with equal probabilities, the entropy density is $S^{calc}(T > T_s) = k_B \ln(3^{n-3})/A = (k_B/A)(n-3)\ln 3$, where k_B is the Boltzmann constant and A is the molecular area of a chain in the liquid surface phase. Assuming further that upon surface freezing the chains assume an all-*trans* conformation, and since all conformational degrees of freedom freeze out, $S^{calc}(T < T_s) \approx 0$. We then recover the linear relation $\Delta S_s^{calc} = S^{calc}(T > T_s) - S^{calc}(T < T_s) = (k_B/A)(n-3)\ln 3$. Since the minimal molecular area is that of close-packed extended alkane molecules, $A \sim 20$ Å^2, the upper limit of the entropy loss upon SF in a melt is $\Delta S_s^{calc\text{-}max} = (k_B/20\ \text{Å}^2)(n-3)\ln 3 = 0.0758(n-3)$ mJ/(m^2 K). As seen in Figure 4b (solid line), this expression has the right linear n dependence, and even a slope very close to the measured $\Delta S_s(n)$ for SF in alkane melts (green symbols and dashed line). However, it still overestimates the measured values. This is not surprising, considering the severe assumptions made, for example, approximating the (unknown) larger molecular area in the liquid phase by that of the solid. Also, the SF layer may have defects, chain-end *gauche* conformations, reduced order near grain boundaries, and so forth, all of which reduce the actual $\Delta S_s(n)$.

These consideration hold to a larger extent for our more complex system. The same-slope linear dependence is demonstrated in Figure 4b by the dash-dot line for STAB, calculated from the ΔS_s^{calc} expression above. This curve lies below the solid line of the melts, due to the larger liquid-phase molecular area, A = 23.4 Å^2, derived from our X-ray measurements in ref 34. Note that in our LG films additional interactions come into play, for example, that of the surfactant's aqueous-surface-confined TMA^+ headgroup with the alkanes, the interchange energy (see below), and so forth, which restrict the mixed LG film's ability to crystallize perfectly, and thus inhibit a realization of the full theoretical ΔS_s^{calc}. Indeed, Figure 4b shows that while for TTAB and STAB bilayers (black and red symbols) the measured $\Delta S_s(n)$ does vary linearly with a slope very close to that of ΔS_s^{calc} for our system (black dash-dot line), and also that of alkane melts (green dashed line), the magnitude of the measured ΔS_s is only about ∼80% of the ΔS_s^{calc} predicted by the simple model above. This agreement may, however, still be considered satisfactory in view of simplifications made.

The most important observation emerging from Figure 4 is that all measured ΔS_s of our system do not exceed the corresponding values measured for SF of alkane melt, where a single crystalline monolayer forms at the surface. We can therefore safely conclude that, in our system, the surface freezing of the LG film also produces only a single crystalline layer for all n, m, and c studied here, in both monolayer and bilayer phases, and that this monolayer is less ordered than that formed on alkane melts. Moreover, the m-independence of ΔS_s in the bilayer phase and its strong m-dependence in the monolayer phase imply that the frozen monolayer of the bilayer phase consists purely of alkanes, while that of the monolayer phase is a mixture of alkanes and surfactant tails. These conclusion are strongly supported by our X-ray measurements, presented and discussed in ref 34.

The Phase Diagram and Its Modeling. *The Measured Phase Diagram.* The surface phase diagrams of the alkanes and surfactants studied here, constructed from the measured T_s values, are shown in Figure 5. For CTAB, they agree closely with the values measured at the same surfactant concentrations

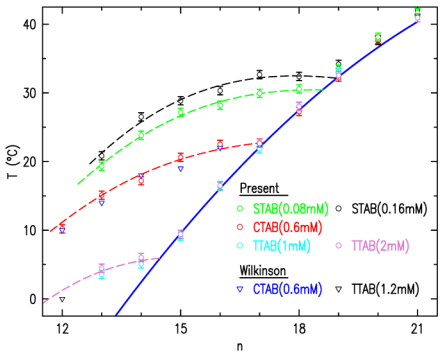

Figure 5. Surface freezing temperatures T_s measured in this study (circles), and by Wilkinson et al.[28] (triangles), for the indicated surfactants, concentrations and alkane lengths n. Dashed lines are fits to the measured T_s by the mixtures-theory-based thermodynamic model discussed in the text. The thick blue line denotes the bulk freezing temperatures T_b. To avoid the odd−even effect[1] in T_b, values for even n, which freeze into a crystalline phase, were interpolated from those of odd n, which freeze into the same rotator phase as the LG films.

dx.doi.org/10.1021/la501567s | *Langmuir* 2014, 30, 8000−8009

by Wilkinson et al.[28] The measured T_s values are observed to exceed T_b for all $n \leq m + 1$, and coincide with T_b within the experimental uncertainty for larger n. This is consistent with our previous CTAB measurements[27] (also included in Figure 5 for completion), where the transition into the bilayer regime occurs at $n = 18$. Thus, the same generic phase diagram is observed for all surfactants: at $T > T_s > T_b$ (for $n \leq m + 1$) or $T > T_s = T_b$ ($n \geq m + 2$), 3D liquid alkane lenses coexist at the surface with a 2D liquid LG film. In the wedge left of $n \leq m + 1$, bound from above by T_s and below by T_b, 3D liquid alkane lenses coexist with a 2D solid LG film. Below T_b, 3D solid alkane lenses coexist with a 2D solid LG film for all n. The consequent range of surface to bulk freezing, $\Delta T = T_s - T_b$, increases fast with decreasing n reaching tens of degrees Celsius for the lowest n that were reachable in this study. This topology is very different from that of the phase diagram of surface freezing in alkane melts, where ΔT increases from zero at $n = 14$ with increasing n, saturates at $\Delta T \approx 3$ °C for $n = 20$, and reduces to zero at $n = 52$. The different topology implies different interactions, and a different interaction balance which determines the phase boundaries in the two systems, as we discuss below.

Thermodynamic Model for Phase Boundaries. The phase behavior and the boundaries observed can be explained within a simple thermodynamic model based on the theory of mixtures,[41,42] and used successfully to account for the universal phase behavior of mixtures of different-length, but same-species, chain molecules.[12,27] For the liquid phase of our LG film, at $T > T_s$, both the alkane molecules and the surfactant tails are flexible and kinked (containing *gauche* configurations), and thus, the LG film can be assumed to be an ideal mixture, neglecting the very small mixing enthalpy expected. The surfactant headgroups reside in the water, so that the hydrophobic surfactant alkyl chains are confined to the upper half-space, and their orientation is distributed broadly around the surface-normal; these restrictions reduce the surfactant entropies as compared to alkanes of the same lengths. The surfactants are then represented by alkanes of an effective noninteger chain length m_{eff}. The free energy per mole, F^l, includes, therefore, only that of the components and their mixing entropy:[12]

$$F^l = \phi f^l_{m_{eff}} + (1-\phi) f^l_n + k_B T[\phi \ln(\phi) + (1-\phi)\ln(1-\phi)] \quad (1)$$

where $f^l_i = \varepsilon^l_i - TS^l_i$ is the molar free energy, and ε^l_i and S^l_i are the molar energy and molar entropy, respectively, of a liquid melt of pure C_i, with $i = n, m_{eff}$. ϕ and $(1-\phi)$ are the mole fractions of surfactants and alkanes, respectively, within the LG film. In the SF phase, $T \leq T_s$, all chains are rigid, extended, and parallel to each other. Thus, replacing surfactant chains by alkanes entails a molar free energy cost of ω, the interchange energy.[12,42] The frozen layer is treated now as a strictly regular mixture, with a free energy:

$$F^s = x f^s_{m_{eff}} + (1-x) f^s_n + k_B T[x \ln(x) + (1-x)\ln(1-x)] + \omega x(1-x) \quad (2)$$

where $f^s_i = \varepsilon^s_i - TS^s_i$ is the molar free energy, and ε^s_i and S^s_i are the energy and entropy, respectively, of pure solid C_i. The last term in eq 2 is the interchange energy in the zeroth-order approximation (nearest neighbor interactions only) of the strictly regular mixtures theory.[12,42] Note that x denotes the surfactant chains' molar fraction in the solid phase, which is not a priori equal to that in the liquid phase, ϕ. At the solid–liquid coexistence temperature, T_s, the chemical potentials derived from F^l and F^s must be equal independently for each component, yielding:

$$T_s = \frac{T_{b,n}\Delta S_n - \omega x^2}{\Delta S_n + k_B \ln[(1-x)/(1-\phi)]} \quad (3)$$

$$T_s = \frac{T_{b,m_{eff}}\Delta S_{m_{eff}} - \omega(1-x)^2}{\Delta S_{m_{eff}} + k_B \ln[x/\phi]} \quad (4)$$

where we employed the equality of the solid and the liquid molar free energy of each of the *pure* components at their corresponding melting temperature to substitute $\varepsilon^l_i - \varepsilon^s_i = T_{b,i}\Delta S_i$.

Equations 3 and 4 yield the surface freezing onset temperatures T_s of a LG film, in terms of the thermodynamical properties of the constituents of the film, the n-length alkane, and the surfactant, considered here to be an m_{eff}-length alkane.

Monolayer Composition. To obtain the interchain interaction ω between alkanes and surfactants, we solve eqs 3 and 4 for x and T_s, at each combination of m_{eff} and n; m_{eff} and ω are tuned to make the resulting $T_s(n)$ fit the experimental data (Figure 5). Literature values[1,7] are used for the pure-alkane freezing temperatures $T_{b,i}$ and the corresponding entropy losses ΔS_i; polynomial interpolations of $T_{b,m_{eff}}$ and $\Delta S_{m_{eff}}$ are employed for noninteger m_{eff}. In all fits, we set $\phi = 0.8$, based on the film thickness values with and without alkanes as refined in the X-ray analysis presented in the accompanying paper.[34] An accurate determination of ϕ, or the related surface excess of the surfactant molecules Γ, is not straightforward, even for alkane-free surfactant solution surfaces. Several methods have been used in the literature for such determinations, employing, respectively, measurements of surface tension,[36,43] neutron reflection,[43] and ellipsometry and nonlinear optical spectroscopy.[44] The results obtained from the three methods for the same solutions generally agree reasonably with each other, considering the complexity of the analysis and its model dependence, as discussed in refs 43 and 45. However, such results are available only for very few points in the (m,T,c) space of interest: mostly near the critical micelle concentration (cmc), at room temperature, and for DTAB to CTAB only. Moreover, they address only alkane-free surfaces, while the solution of eqs 3 and 4 requires ϕ values for alkane-including LG films. Thus, our present n-, m-, and c-independent choice of ϕ is justifiable by the unavailability of more reliable experimental data.

Previous studies[27] estimated ϕ by assuming for the LG film the same fractional surface coverage by surfactants as that of the alkane-free surface of a surfactant solution having the same bulk concentration. Our present, more systematic X-ray studies allow a more reliable estimate of ϕ to be obtained, based on direct comparison between the X-ray derived[34] structures of alkane-free and alkane-coated water interfaces, for several different alkanes and surfactants; the new ϕ value necessitated some details of the thermodynamical model presented above to be revised from those of the previous work.[27]

To increase the reliability of fitted ω and m_{eff}, we constrain ω to scale as $(\Delta n/\bar{n})^2$, where $\Delta n = n - m_{eff}$ is the length mismatch between the surfactant tail and the alkane, and $\bar{n} = (n + m_{eff})/2$

dx.doi.org/10.1021/la501567s | Langmuir 2014, 30, 8000–8009

is the average of these two lengths. This scaling was shown to dominate the surface freezing in binary mixtures of same-species but different-length alkanes and alcohols,[12] and in LG films of alkanes on CTAB solution.[27] While for SF in alkane melts, $\omega = \beta(\Delta n/\overline{n})^2$, with no energetic penalty for mixing of alkanes of identical chain lengths, for the LG films a constant term needs to be included to account for the interaction of the surfactant's TMA^+ headgroup and the alkane:

$$\omega = a + b(\Delta n/\overline{n})^2 \quad (5)$$

Thus, within this model, the STAB differs thermodynamically from a $C_{m_{eff}}$ molecule only by the headgroup interaction energy a. This allows all the available experimental T_s values for LG monolayers ($n \leq m + 1$) to be reproduced by tuning of a, b, and m_{eff}. Note the excellent agreement of the theoretical fits (dashes) with the experimental data (symbols) in Figure 5; the corresponding ω, m_{eff} and a values are shown in Figure 6a, b,

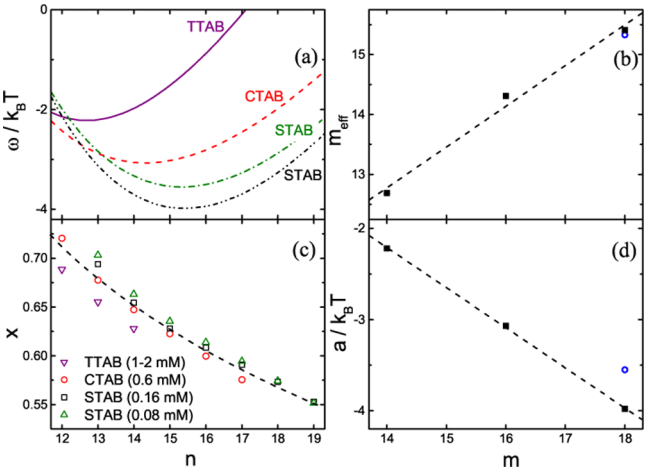

Figure 6. (a) The interchange energy ω, obtained from fits of eqs 3 and 4 to the measured T_s of LG monolayers, for the three surfactants at bulk concentrations of $c \approx 0.6$cmc. For comparison, ω at $c \approx 0.3$cmc of STAB is shown in a green dash-dot curve; the T_s values for TTAB, obtained at several different concentrations, are merged, as explained in the text. Note that all values are negative, as discussed in the text. The minimum position of $\omega(n)$ corresponds to the effective chain length of the surfactant, m_{eff}. This is shown in (b) and is lower by ~2 carbon units than the actual tail length of the surfactant. The open circle in (b) corresponds to STAB, at $c \approx 0.3$cmc. (c) The molar fraction of the alkyl tails in the solid phase, x, as obtained from the solution of eqs 3 and 4. Note the decrease of x with n, and the near-coincidence of the values for different surfactants and concentrations. (d) The constant energy term a, associated with the TMA^+ headgroup contribution to the interchange energy ω (see text) depends linearly on the tail length of the surfactant; symbols are the same as in (b).

and d. For TTAB, only two $T_s(n)$ points could be measured within the monolayer phase. For these points to support a fit by the model, we have supplemented them by the additional single point measured by Wilkinson et al.[28] for $n = 12$ at a slightly different concentration. TTAB data obtained at different concentrations were, in this case, sufficiently close together; therefore, these data were merged for the fit.

In addition to ω, this formalism yields also the surfactant concentration in the solid LG films x. This further constrains the parameters' space, as x values larger than ~0.66 are geometrically prohibited, due to the ~32 Å^2 cross-sectional area of the TMA^+ headgroup.[46] Our resulting x values, shown in Figure 6c, satisfy this geometrical constraint, except for a couple of points for the lowest n, which slightly exceed this limit. Interestingly, x values obtained with different surfactants and surfactant concentrations almost coincide, providing further support to our formalism, where the internal degrees of freedom of surfactant headgroups are not explicitly taken into account. Finally, the convergence of x to its geometrical limit $x \approx 0.66$ for $n = 12$ suggests that the current mechanism is unable to induce freezing of LG films for shorter alkanes; indeed, no freezing transitions were observed in preliminary experiments, where $n < 12$.

The Interchange Energy ω. For all alkane and surfactant combinations studied, the effective chain length of the surfactant m_{eff} is smaller than the actual length of the alkyl tail [see Figure 6b] by ~2 carbon units. This discrepancy can be assigned to the length taken up by the van der Waals (vdW) radii of the alkane's terminal CH_3 and of the surfactant's TMA^+ headgroups. The optimal length match of an extended alkane molecule to an extended C_mTAB tail (corresponding to the minimum point in Figure 6a) should therefore occur for n shorter than m by 1.5−2.5 methylene groups. This was indeed demonstrated experimentally for water-supported films of alkanol−CTAB mixtures,[47] and for LG films of alkanes both on the surface of CTAB solutions[27] and at the interface between alkane and solution bulks.[25,26] A contribution from water molecules rising into the hydrophobic region of the chains is also possible.[48,49] The optimal shift for CTAB was found to be ~2 carbons,[25] like in our case. Finally, with the free energy of the surfactant taken in our formalism to be equal to that of an effective alkane of m_{eff} carbon units, the discrepancy between m and m_{eff} also accounts for the liquid entropy reduction of the surfactant, compared to an alkane. Indeed, the TMA^+ headgroups, restricted to reside in water, induce partial alignment of the alkyl tail. This alignment is likely to extend to a distance of ~2 carbon units from the headgroup, in agreement with the fitted m_{eff} value being slightly lower than the actual m. Future measurements, on a wider range of surfactant lengths should allow to verify whether this value is indeed m-independent, as found here.

The values of a, b, and m_{eff} obtained here for LG films on TTAB, CTAB, and STAB solutions are listed in Table 2.

Table 2. Parameter Values of eq 5 Obtained from Fits to the Experiment-Derived ω[a]

surf	conc, mM	a, k_BT	b, k_BT	m_{eff}
TTAB	1−2	−2.2(1)	25(1)	12.7(1)
CTAB	0.6	−3.1(1)	21(1)	14.3(1)
STAB	0.08	−3.6(1)	26(2)	15.3(1)
STAB	0.16	−4.0(1)	30(1)	15.4(1)

[a] a and b are in units of k_BT. m_{eff} denotes the chain length of the effective alkane molecule, which represents the alkyl tail of the surfactant in our thermodynamical model. Numbers in parentheses denote uncertainties in the value's last digit.

Interestingly, while b varies randomly within 20% of the average $25k_BT$ value for all concentrations and surfactant chain lengths, a scales linearly in m, as demonstrated in Figure 6d. Moreover, the b values obtained are all positive, indicating that the second term in eq 5 is repulsive and drives toward a segregation of the two species comprising the film. However, a is negative, that is, attractive, and thus drives toward a mixed LG film. This effective attraction arises from the Coulombic repulsion of the

dx.doi.org/10.1021/la501567s | Langmuir 2014, 30, 8000−8009

charged TMA^+ headgroups. Moreover, a close approach of the tails of two surfactants, favored by their van der Waals attraction, is sterically prohibited by the presence of the bulky TMA^+ headgroups. At the same time, a close approach of an alkane and a surfactant *is* allowed, enhancing the alkane−TMA^+ attraction. The total contribution due to maximization of van der Waals contacts between the alkyl tails is larger for the longer surfactants; this explains the increase in the absolute value of a for STAB, compared to CTAB and TTAB (see Figure 6d). Importantly, as evidenced by the slope of $a(m)$, this increase is quite modest, $(0.44 \pm 0.01)\ k_BT$ per CH_2 group, 6-fold smaller than the typical cohesion energy of hydrocarbons, $\sim 2.8\ k_BT$ per CH_2 group.[32] The magnitudes of the two opposite-signed a and b are such that ω obtained here is always negative, and thus favors a mixed LG film. This is in contrast with SF of binary melts of alkanes[12] where, in the absence of an a term, ω is always repulsive and invariably drives toward phase separation.

Note that the energetic penalty for the length mismatch in LG films ($b \approx 25 k_BT$) is roughly twice that of a surface frozen layer in alkane mixture melts[12] ($b \approx 12 k_BT$). One can speculate that this arises from the LG film being confined to the aqueous surface, which is an impenetrable boundary for the alkanes. Thus, the alkane extends from this boundary up, and the extra carbons of the longer chain (be it the alkane or the surfactant) reside all on the vapor side of the LG film. By contrast, in the SF layer of alkane mixture melts, a molecule may extend into the underlying bulk melt, providing two mismatch regions, one at each interface of the SF layer, with half the total chain lengths' difference protruding from each interface. With the quadratic Δn dependence, a trivial calculation shows that the resultant ω is only half that of the surface frozen LG film where the full difference protrudes into the vapor side. The agreement of this argument with the measured values strengthens the validity of the model used here and the choice of $\phi = 0.8$ employed.

As discussed above, the current model predicts x to reach its geometrical limit for $n = 12$. Interestingly, in agreement with this prediction, the lowest n values for which we were able to observe SF were $n = 12$ for CTAB and $n = 13$ for the two concentrations of STAB and TTAB. However, while entirely consistent with the behavior of x in our model, the disappearance of SF may as well be due to a combination of several effects. In particular, for STAB and CTAB, the variation of the bulk surfactant concentration with temperature must be considered. As Figure 5 demonstrates for STAB, a reduction of the surfactant's bulk concentration reduces T_s, diminishing the temperature interval over which SF occurs. Continuing to reduce the surfactant's bulk concentration would lead to a concomitant reduction in the existence n-range of SF in the phase diagram, until a low concentration limit is reached where the SF effect vanishes. This was indeed observed for LG films of hexadecane on DTAB solution.[50] In our case, the bulk concentration decrease is caused by the sharp reduction in the bulk surfactant solubility as T_s decreases with n. As Figure 5 demonstrates, T_s decreases from ~20 °C for $n = 13$ to ~10 °C for $n = 12$. While the solubility limits for our nominal concentration are not known, these concentrations are close enough to the cmc to allow obtaining at least a feeling for the solubility from the position of T_s relative to the Krafft point, which is the solubility limit at the cmc. STAB's Kraft point is[51] $T_K = 35$ °C, far above T_s ($n = 13$). We suggest therefore that SF is not observed for $n \leq 12$, since upon cooling the sample toward $T_s \approx 10$ °C the surfactant sufficiently precipitates from the solution to deplete it to a level which does not support the emergence of SF. Although this effect was not observed in situ, we did observe STAB precipitation in solutions left to stand for extended periods of time at temperatures below 20 °C. Similar considerations may explain why we did not observe SF for $n \leq 11$ on a CTAB solution, where the Krafft point is[51] $T_K = 25$ °C, and the expected $T_s \approx 3$ °C.

Surface Coverage by the Surfactant. To obtain the coverage, Γ, of the alkane-free solution's surface by surfactant molecules and compare these values to estimates based on our X-ray experiments,[34] we measured the fixed-temperature concentration dependence of γ for TTAB and STAB solutions at several temperatures. These measurements are shown in Figure 7. $\gamma(\ln c)$ yields the surface coverage Γ through the

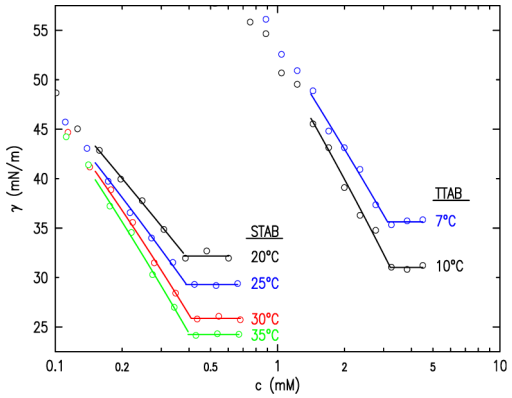

Figure 7. Measured (symbols) and fitted (lines) concentration dependence of γ at the indicated temperatures. The curves' break points mark the cmc.

Gibbs equation:[29,36] $\Gamma = -[1/(2RT)]/[d\gamma/d(\ln c)]$, where $R = 8.31451$ J/(mol K) is the molar gas constant. The Γ values obtained here, Figure 8a, conform to the upper limit of $\Gamma \lesssim 5$ $\mu M/m^2$, derived from the ~32 $Å^2$ cross-sectional area of the bare TMA^+ headgroup,[46] although the real cross section may be somewhat larger due to the headgroup's hydration shell. The results also agree with the values obtained for CTAB by Wilkinson et al.,[28] as also with our X-ray measurements presented in the next paper.[34]

The inflection point of $\gamma(\ln c)$ yields the cmc's, which are plotted in Figure 8b. While in principle extraction of both Γ and the cmc from the $\gamma(\ln c)$ curves requires a careful fitting of $\gamma(\ln c)$ below the cmc by a polynomial rather than a straight line,[43] no significant difference was found in practice between the values derived from our data by both methods. The cmc results are in good agreement with, and extend the temperature range of, previous measurements, albeit with larger experimental uncertainties.

SUMMARY AND CONCLUSIONS

The measurements above provide a detailed description of the thermodynamics of surface freezing occurring at T_s in a mixed LG film of n-long alkanes and m-long tails of C_mTAB surfactants, at the free surface of the surfactant solution. When compared with surface freezing in alkane melts,[7] the entropy loss upon freezing indicates that the surface freezing occurs here in a single monolayer. The measured T_s values are used to construct the phase boundaries between the surface phases of the LG film. We find that the bulk freezing line of the

dx.doi.org/10.1021/la501567s | Langmuir 2014, 30, 8000−8009

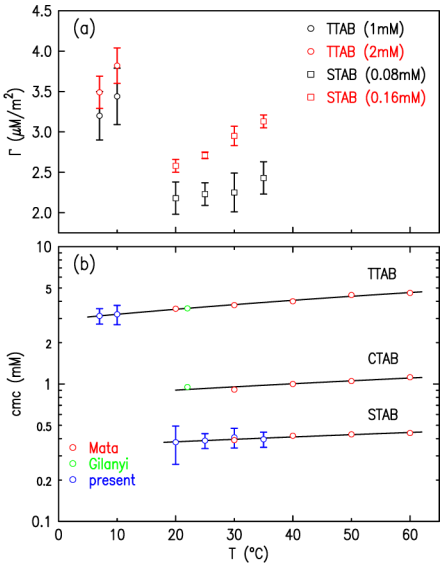

Figure 8. (a) Measured (symbols) surface coverage by surfactant molecules without alkanes, calculated from the $\gamma(c)$ curves in Figure 7 for the surfactants, concentrations, and temperatures indicated. (b) cmc values derived from the $\gamma(c)$ curves in Figure 7, compared with measurements of Mata et al.[52] and Gilanyi et al.[36] Linear fits (lines) to all measured points for each surfactant are also shown.

alkanes preempts the surface-freezing line for $n \geq m + 2$ for all m studied here. A simple thermodynamic model where the mixed LG film is taken to be an ideal mixture in the liquid phase above T_s and a strictly regular mixture below T_s is found to account well for the observed phase boundaries. It demonstrates that the transition is dominated by the interchange energy term, ω, which exhibits attraction between the two species of the mixture, alkane and surfactant tail, for all n and m studied here. This is in contrast with SF in binary mixtures of alkane where ω is always positive and unlike species always repel each other. Our model also predicts the preemption of the SF line by the bulk freezing line of the alkane for large n values (above $n = m + 1$), as well as the inability of current mechanism to support the freezing of LG films for short alkanes, $n \lesssim 12$. These two limits seem to be indeed observable in experiment, albeit the proximity of the T_s values of low n to the Kraft points of the surfactants does not allow a confident validation of the lower n-limit of SF in the systems studied here.

These main findings of the study presented here of surfactant-induced SF in mixed LG films still lack one important component: the elucidation of the structure of the frozen and liquid film, above and below the temperature boundary T_s and above and below the alkane length boundary of $n = m + 1$, imposed by the surfactant tail's length. This elucidation requires X-ray studies by surface-specific synchrotron X-ray diffraction methods, which are detailed in the next paper.[34]

AUTHOR INFORMATION

Corresponding Authors

*E-mail: deutsch@mail.biu.ac.il.

*E-mail: ocko@bnl.gov.

Present Addresses

[‖]L.T.: Nova Measuring Instruments Ltd., Rehovot, Israel.

[⊥]Z.S.: Intel (Israel) Ltd., Kiryat Gat, Israel.

Author Contributions

[§]S.Y. and E.S. contributed equally to this work.

Notes

The authors declare no competing financial interest.

ACKNOWLEDGMENTS

Support by the U.S.-Israel Binational Science Foundation, Jerusalem is gratefully acknowledged (M.D.). This research was supported by the U.S. Department of Energy, Office of Basic Energy Sciences, Materials Sciences and Engineering Division, under Contract No. DE- AC02-98CH10886 (B.M.O.).

REFERENCES

(1) Small, D. M. *The Physical Chemistry of Lipids*; Plenum: New York, 1986.

(2) Sirota, E. B.; Herhold, A. B. Transient phase-induced nucleation. *Science* **1999**, *283*, 529−532.

(3) Kumar, M. V.; Prasad, S. K.; Rao, D. S. S. Confinement-driven weakening of the rotator phase transitions in an alkane through a possible tricritical point. *Langmuir* **2010**, *26*, 18362−18368.

(4) Sirota, E. B.; Kink, H. E.; Singer, D. M.; Shao, H. H. Rotator phases of the normal alaknes-an X-ray scattering study. *J. Chem. Phys.* **1993**, *98*, 5809−5824.

(5) Earnshaw, J.; Hughes, C. Surface-induced phase-transition in normal alkane fluids. *Phys. Rev. A* **1992**, *46*, 4494.

(6) Wu, X. Z.; Ocko, B. M.; Sirota, E. B.; Sinha, S. K.; Deutsch, M.; Cao, G. H.; Kim, M. W. Surface tension measurements of surface freezing in liquid normal alkanes. *Science* **1993**, *261*, 1018.

(7) Ocko, B. M.; Wu, X. Z.; Sirota, E. B.; Sinha, S. K.; Gang, O.; Deutsch, M. Surface freezing in chain molecules: Normal alkanes. *Phys. Rev. E* **1997**, *55*, 3164.

(8) Frenken, J. W. M.; van-der Veen, J. F. Observation of surface melting. *Phys. Rev. Lett.* **1985**, *54*, 134−137.

(9) Schoeder, S.; Reichert, H.; Schroeder, H.; Mezger, M.; Okasinski, J. S.; Honkimaeki, V.; Bilgram, J.; Dosch, H. Radiation-Induced Premelting of Ice at Silica Interfaces. *Phys. Rev. Lett.* **2009**, *103*, 095502.

(10) Shinohara, Y.; Kawasaki, N.; Ueno, S.; Kobayashi, I.; Nakajima, M.; Amemiya, Y. Observation of the transient rotator phase of n-hexadecane in emulsified droplets with time-resolved two-dimensional small- and wide-angle X-ray scattering. *Phys. Rev. Lett.* **2005**, *94*, 097801.

(11) Gruener, S.; Huber, P. Spontaneous imbibition dynamics of an n-alkane in nanopores: Evidence of meniscus freezing and monolayer sticking. *Phys. Rev. Lett.* **2009**, *103*, 174501.

(12) Sloutskin, E.; Wu, X. Z.; Peterson, T. B.; Gang, O.; Ocko, B. M.; Sirota, E. B.; Deutsch, M. Surface freezing in binary mixtures of chain molecules. I. Alkane mixtures. *Phys. Rev. E* **2003**, *68*, 031605.

(13) Mechler, S.; Pershan, P. S.; Yahel, E.; Stoltz, S. E.; Shpyrko, O. G.; Lin, B.; Meron, M.; Sellner, S. Self-Consistent Interpretation of the 2D Structure of the Liquid $Au_{82}Si_{18}$ Surface: Bending Rigidity and the Debye-Waller Effect. *Phys. Rev. Lett.* **2010**, *105*, 186101.

(14) Sirota, E. B.; Wu, X. Z.; Ocko, B. M.; Deutsch, M. What drives the surface freezing in alkanes? *Phys. Rev. Lett.* **1997**, *79*, 531.

(15) Leermakers, F. A. M.; Cohen-Stuart, M. A. Self-consistent-field lattice gas model for the surface ordering transition of *n*-hexadecane. *Phys. Rev. Lett.* **1996**, *76*, 82−85.

(16) Tkachenko, A.; Rabin, Y. Fluctuation-stabilized surface freezing of chain molecules. *Phys. Rev. Lett.* **1996**, *76*, 2527−2530.

(17) Colussi, A. J.; Hoffmann, M. R.; Tang, Y. Conformational disorder binds *n*-alkanes into surface monolayers above the normal freezing point. *Langmuir* **2000**, *16*, 5213−5217.

(18) Schlangen, L. J. M.; Koopal, L. K.; Lyklema, J. Self-consistent-field description of *n*-alkanes in bulk and at the liquid−vapor interface. *J. Phys. Chem.* **1996**, *100*, 3607−3616.

(19) Li, H. Z.; Yamamoto, T. The surface-ordered phase of *n*-nonadecane: A molecular dynamics simulation. *J. Chem. Phys.* **2001**, *114*, 5774−5780.
(20) Zhang, Y.; Ou-Yang, Z. C.; Iwamoto, M. Surface freezing in normal alkanes: A statistical physics approach. *J. Chem. Phys.* **2006**, *124*, 214906.
(21) Holzwarth, A.; Leporatti, S.; Riegler, H. Molecular ordering and domain morphology of molecularly thin triacontane films at SiO_2/air interfaces. *Europhys. Lett.* **2000**, *52*, 653−659.
(22) Kusmin, A.; Gruener, S.; Henschel, A.; Holderer, O.; Allgaier, J.; Richter, D.; Huber, P. Evidence of a sticky boundary layer in nanochannels: A neutron spin echo study of *n*-hexatriacontane and poly(ethylene oxide) confined in porous silicon. *J. Phys. Chem. Lett.* **2010**, *1*, 3116−3121.
(23) Ocko, B. M.; Hlaing, H.; Jepsen, P. N.; Kewalramani, S.; Tkachenko, A.; Pontoni, D.; Reichert, H.; Deutsch, M. Unifying interfacial self-assembly and surface freezing. *Phys. Rev. Lett.* **2011**, *106*, 137801.
(24) Mitrinovic, D. M.; Tikhonov, A. M.; Li, M.; Huang, Z. Q.; Schlossman, M. L. Noncapillary-wave structure at the water-alkane interface. *Phys. Rev. Lett.* **2000**, *85*, 582−585.
(25) Lei, Q.; Bain, C. D. Surfactant-induced surface freezing at the alkane-water interface. *Phys. Rev. Lett.* **2004**, *92*, 176103.
(26) Tamam, L.; Pontoni, D.; Sapir, Z.; Yefet, S.; Sloutskin, E.; Ocko, B. M.; Reichert, H.; Deutsch, M. Modifcation of deeply buried hydrophobic interfaces by ionic surfactants. *Proc. Natl. Acad. Sci. U.S.A.* **2011**, *108*, 5522−5525.
(27) Sloutskin, E.; Sapir, Z.; Bain, C. D.; Lei, Q.; Wilkinson, K. M.; Tamam, L.; Deutsch, M.; Ocko, B. M. Wetting, mixing, and phase transitions in Langmuir-Gibbs films. *Phys. Rev. Lett.* **2007**, *99*, 136102.
(28) Wilkinson, K. M.; Lei, Q.; Bain, C. D. Freezing transitions in mixed surfactant/alkane monolayers at the air-solution interface. *Soft Matter* **2006**, *2*, 66.
(29) Wilkinson, K.; Bain, C.; Matsubara, H.; Aratono, M. Wetting of surfactant solutions by alkanes. *ChemPhysChem* **2005**, *6*, 547−555.
(30) Bonn, D.; Eggers, J.; Indekeu, J.; Meunier, J.; Rolley, E. Wetting and spreading. *Rev. Mod. Phys.* **2009**, *81*, 739−805.
(31) Matsubara, H.; Aratono, A.; Wilkinson, K.; Bain, C. Lattice model for the wetting transition of alkanes on aqueous surfactant solutions. *Langmuir* **2006**, *22*, 982−988.
(32) Israelachvili, J. *Intermolecular and surface forces*, 2nd ed.; Academic Press: London, 1992.
(33) McKenna, C. E.; Knock, M. M.; Bain, C. D. First-order phase transition in mixed monolayers of hexadecyltrimethylammonium bromide and tetradecane at the air−water interface. *Langmuir* **2000**, *16*, 5853−5855.
(34) Yefet, S.; Sloutskin, E.; Tamam, L.; Sapir, Z.; Deutsch, M.; Ocko, B. M. Surfactant-induced phases in water-supported alkane monolayers: II. Structure. *Langmuir* **2014**, DOI: 10.1021/la501589t.
(35) Ohtomi, E.; Takiue, T.; Aratono, M.; Matsubara, H. Freezing transition of wetting film of tetradecane on tetradecyltrimethylammonium bromide solutions. *Colloid Polym. Sci.* **2010**, *288*, 1333−1339.
(36) Gilanyi, T.; Varga, I.; Stubenrauch, C.; Meszaros, R. Adsorption of alkyl trimethylammonium bromides at the air/water interface. *J. Colloid Interface Sci.* **2008**, *317*, 395−401.
(37) Vollhardt, D.; Fainerman, V. B. Characterisation of phase transition in adsorbed monolayers at the air/water interface. *Adv. Colloid Interface Sci.* **2010**, *154*, 1−19.
(38) Gaines, G. L. *Insoluble Monolayers at Liqid Gas Interface*; Wiley: New York, 1966.
(39) Gang, O.; Ocko, B. M.; Wu, X. Z.; Sirota, E. B.; Deutsch, M. Surface freezing in hydrated alcohol melts. *Phys. Rev. Lett.* **1998**, *80*, 1264−1267.
(40) deGennes, P. G. *Scaling Concepts in Polymer Physics*; Cornell University Press: Ithaca, NY, 1979.
(41) R. Defay et al., *Surface Tension and Adsorption*; Wiley: New York, 1966.
(42) Guggenheim, E. A. *Mixtures*; OUP: Oxford, 1952.
(43) Simister, E. A.; Thomas, R. K.; Penfold, J.; Aveyard, B. P.; Blinks, P.; Cooper, P.; Fletcher, P. D. I.; Sokolowski, A. Comparison of neutron reflection and surface tension measurements of the surface excess of tetradecyltrimethylammonium bromide layers at the air/water interfacxe. *J. Phys. Chem.* **1992**, *96*, 1383−1388.
(44) Bell, G. R.; Manning-Benson, S.; Bain, C. D. Effect of chain length on the structure of monolayers of alkyltrimethylammonium bromides (C_nTABs) at the air−water interface. *J. Phys. Chem. B* **1998**, *102*, 218−222.
(45) Battal, T.; Shearman, G. C.; Valkovska, D.; Bain, C. D.; Darton, R. C.; Eastoe, J. Determination of the dynamic surface excess of a homologous series of cationic surfactants by ellipsometry. *Langmuir* **2003**, *19*, 1244−1248.
(46) Janczuk, B.; Zdziennicka, A.; Jurkiewicz, K.; Wojcik, W. The surface free energy and free energy of adsorption of cetyltrimethylammonium bromide. *Tenside, Surfactants, Deterg.* **1998**, *35*, 213−217.
(47) Casson, B. D.; Bain, C. D. Phase transitions in mixed monolayers of cationic surfactants and dodecanol at the air−water interface. *J. Phys. Chem. B* **1999**, *103*, 4678−4686.
(48) Thomas, R. K. Neutron reflection from liquid interfaces. *Ann. Rev. Phys. Chem.* **2004**, *55*, 391−426.
(49) Tarek, M.; Tobias, D. J.; Klein, M. L. Molecular-dynamics simulation of tetradecyltrimethylammonium bromide monolayers at the air-water-interface. *J. Phys. Chem.* **1995**, *99*, 1393−1402.
(50) Matsubara, H.; Ohtomi, E.; Aratono, M.; Bain, C. D. Wetting and freezing of hexadecane on an aqueous surfactant solution: Triple point in a 2-D film. *J. Phys. Chem. B* **2008**, *112*, 11664.
(51) Vautier-Giongo, C.; Bales, B. L. Estimate of the ionization degree of ionic micelles based on Krafft temperature measurements. *J. Phys. Chem. B* **2003**, *107*, 5398−5403.
(52) Mata, J.; Varade, D.; Bahadur, P. Aggregation behavior of quaternary salt based cationic surfactants. *Thermochim. Acta* **2005**, *428*, 147−155.